Zn-air battery with a PEDOT: PSS cathode as a viable option for wearable medical devices

F. IERMANO[1,*], I. BOBINAC[2], P. DONGO[1], V. GALLO[3], H. MACHRAFI[1,4], C.S IORIO[1]

[1]*Université Libre de Bruxelles, Chimie-Physique E.P, Bruxelles, Belgium*

[2]*Politecnico Di Milano, Milan, Italy*

[3]*Università Degli Studi Di Napoli Federico II, Naples, Italy*

[4]*Université de Liège, GIGA-In Silico Medicine, Liège, Belgium*

** Author for correspondence, email: fabio.iermano@ulb.be*

Abstract

For medical sensing devices, such as wound healing patches, it is necessary to provide wearable and long-term usable power supply. This calls for cost-effective, lightweight batteries. We propose here a metal-air battery composed out of a Zn anode and a poly(3,4- ethylene dioxythiophene): poly(styrene sulfonate) (PEDOT: PSS) cathode. A PEDOT: PSS layer was created by film deposition and used as cathode without binders because of its high adhesion. Two film types of different thicknesses were analysed. The effect of a 1-butyl- 3-methylimidazolium octyl sulfate ionic liquid, also reported to act as a stabilizer, on the electric performance has been assessed. The electrodes presented low surface resistivity and a considerable discharge capacity. The results showed that PEDOT: PSS acts properly as an O_2 redox reaction matrix and conducting binder in the air electrode, implying that PEDOT: PSS films are suitable for Zn-Air batteries' cathode. Moreover, we demonstrate a polymer-enabled biocompatible Zn−air battery device with a total thickness of approximately 2 mm, easily to assemble, light-weight and cost-effective.

1. Introduction

The increase of chronic disease, the growing geriatric population, and the burden on healthcare management represented by rural and remote areas push for finding cost-effective and robust e-monitoring devices and concepts [1].

In the last decade, an exponentially increasing trend concerned the development of medical devices designed to comply with specific requirements such as affordability, portability, stability, biocompatibility and connectivity. Examples of those new concepts could be found in the literature under the name of Implanted Medical Devices (IMDs) [2]–[4], low-cost Internet of Medical Things (IoMT) sensors [5].

An open challenge in developing portable devices is represented by the power needed for sensors to record and transmit data. Many solutions have been proposed ranging from in-vivo energy harvesting devices [6]–[8] up to energy storage devices, but no definite technology is eventually available [9]. According to what is reported by Stauss and Homma [10], to power drug delivery systems and muscle stimulators, powers of the order of 10^{-2} mW and a duration of several hours would be sufficient for such devices.

Zn–air batteries have attracted much attention and recently received revived research efforts due to their high energy density, making them a promising candidate for emerging mobile and electronic applications [11]. These batteries possess some desirable features such as a high theoretical energy density, low cost, safety and environmental friendliness [12]. The theoretical energy density of Zn–air is 1086 $Wh \cdot kg^{-1}$, and its operational cost is estimated to be less than 10 $\$ \cdot kW^{-1} \cdot h^{-1}$.

Zn-air batteries face the challenge of having low-cost yet efficient catalysts for the air cathode to promote electrochemical oxygen reactions. Different configurations and materials for the cathode have been explored. Platinum (Pt) catalysts and alloys are the standard but are not cost-effective and scarcely available [13]. Non-

precious metals as metal oxides, transition-metal macrocycles and nitrogen-doped carbon-based materials are also widely used, but they still face sustainability concerns of the possible negative impacts on the environment [14].

Our group considered conductive polymers poly(3,4-ethylenedioxythiophene) (PEDOT) as a material to be integrated as the air cathode for biosafety and low cost. Conductive polymers as PEDOT have high conductivity and electrocatalytic activity for oxygen reduction [15]–[17]. They are already in use in many commercially available technologies, such as organic light-emitting diodes (OLEDs) for screen application, organic thin-film transistors (OTFTs) and organic solar cells (OSCs) [18]. Some PEDOT applications are reported in the literature as part of the air electrode in the metal-air batteries, showing good performances [19], [20].

In the present study, PEDOT: PSS is proposed as the cathode for the Zn-Air battery. A PEDOT: PSS layer was created by film deposition and used as an electrode without binders because of its high adhesion. The influence of the film thickness and of the 1-butyl- 3-methylimidazolium octyl sulfate ionic liquid on the electrodes' electrochemical properties is presented. A discharge test and characterisation of the electrodes is also proposed to assess the battery's functioning and performance. The easiness of assembling, cost-effectiveness and compactness of our system will be given due attention.

2. Materials and method

2.1. Materials

For the preparations of the films, the materials used were: PEDOT: PSS aqueous dispersion (CLEVIOS™ PH 1000) with a solid content between 1.0-1.3 % purchased from Heraeus; 1-butyl-3-methylimidazolium octyl sulfate ionic liquid (≥96% HPLC) from Sigma Aldrich; and Polydimethylsiloxane (PDMS) (DOW SYLGARD 184 Silicone Elastomer Kit) bought from Dow Inc.

For the battery's anode, zinc foil was used with a purity of 99.9% and surface resistance of 5.8 μΩ·cm at room temperature, purchased from Sigma-Aldrich. Whatman Grade 41 filter paper with pore size between 20 to 25 μm as separator and a sterile and filtered phosphate buffered saline (PBS) solution, with pH 7.4, purchased from Sigma-Aldrich, as the electrolyte. 80 μm thick gold foils were employed as connectors, and PLA filament for 3D printers from RS International was modelled to create the mould for hosting the different layers of the battery.

2.2. Preparation PEDOT films and characterisation

Two types of PEDOT: PSS films were formed (thin and thick film) following the procedures proposed by Wang et al. [21]. For every kind of films, one chemical dopant was added in different concentrations to enhance the conductivity properties and find the optimal formulation to be used as the cathode. A 1-butyl- 3-methylimidazolium octyl sulfate ionic liquid (IL) was added to the PEDOT: PSS's aqueous dispersion before annealing, varying the end-product concentration (0 wt%, 15 wt%, 30 wt%, 45 wt% and 60 wt%).

Tests were done to analyse the properties of the films and discriminate the best formulation. Fourier-Transform InfraRed spectrum (FTIR) measurements were recorded using a Jasco FT/IR-6600 spectrometer in ATR mode to assess if the addition of the dopant started any chemical reaction. The PEDOT: PSS films' structures were observed using Hitachi SU-70 scanning electron microscope (SEM), and The Veeco Dektak® 150 Surface Profiler was used to get the thickness and the surface profile of the films. The chemical compositions of the material were recorded with Energy Dispersive X-ray spectroscopy (EDS). The films' conductivity was measured with the Keithley 2400 SourceMeter SMU, allowing for four-probe resistivity measurements.

2.3. Assembly of the stack and testing

The battery was assembled as a sandwich structure. The external parts were the PLA supports modelled in the SolidWorks 2017 software and fabricated using Prusa i3 MK3 3D printer. They were designed with a cavity 0.4 mm deep of 25 mm^2 to host the electrodes ensuring good adhesion of components and grooves for connection terminals. In addition, the cathode's support has also air-flow channels that are necessary to provide air in this metal-air battery. A 80 μm thick gold foil was glued directly to the PLA supports. On one support, a 25 mm^2 Zn foil anode of 0.25 mm thickness was attached, and on the other one, a 25 mm^2 PEDOT: PSS film cathode was deposited. As a separator, 25 mm^2 Whatman Grade 41 filter paper was used, chosen for its flexibility, biodegradability, and precise pore size from 20 to 25 μm. The separator was immersed for 10 minutes in a phosphate buffered saline (PBS) electrolyte. The phosphate buffer saline was chosen as the electrolyte since it can

mimic bodily fluids. The whole setup was held up by 4 PTFE screws mounted through the predesigned holes in supports.

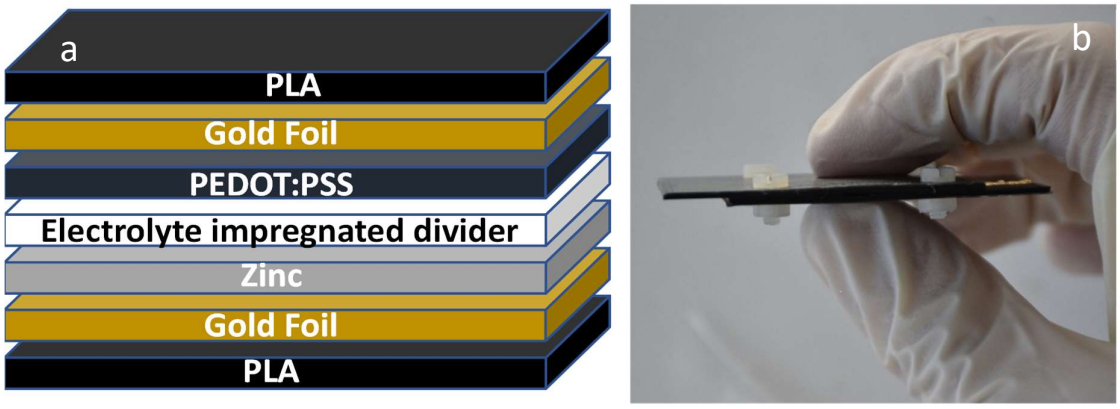

Fig. 1 (a)Layers of the battery; (b) The assembled battery.

Some of the most crucial battery parameters are discharge time, capacity and energy density. All of these could be obtained simply by performing the discharge test. Discharge tests are carried out by applying a constant current on the battery while measuring the potential difference that it generates over time. The discharge time of a battery varies according to the load to which it is subjected, so it is necessary to choose a suitable load. In our work, it was chosen 0.8 mA·cm^{-2} and 1 mA·cm^{-2} (200 µA and 1 mA constant currents). The discharge test was completed with a Keithley 2400 SourceMeter SMU measuring instrument. All the data were recorded using KickStart I-V Characterization software.

After discharge, to analyse the influence on the materials of reaction responsible for the charge generation, post-discharge tests were done. Scanning Electron Microscope (SEM) images and EDS spectra were done for Zn-electrode, PEDOT: PSS electrode and the separator.

3. Results and Discussion

PEDOT: PSS films were created with two thicknesses ~24 µm and ~142 µm, measured with the profilometer. 1-butyl-3-methylimidazolium octyl sulfate ionic liquid was used as dopant in concentrations 0 wt%, 15 wt%, 30 wt%, 45 wt% and 60 wt%. The conductivity was considered to be the discriminant parameter between the films and to choose which is the best formulation and thickness. The resistivity and conductivity can be calculated if the sheet resistance and material thickness are known. This allows for the materials to be electrically characterized, purely by measuring their surface resistivity. The technique for measuring sheet resistance is the four-probe method. This method consists of four electrical probes in a line, with equal spacing between each of the probes. The measurement of surface resistance with this four-probe system operates by applying a current I on the outer two probes and measuring the resultant voltage drop V between the inner two probes. For a uniform spacing $S =$ 7 mm between the probes (with contact diameter of 0.4 mm), and a sheet thickness much smaller than the probe spacing, the sheet resistance is given by $R_s = C\frac{\pi}{ln}\frac{V}{I}$, where we introduced a geometrical correction factor C. The geometrical correction factor equals unity when the sample dimensions (length L and width W) are significantly larger than the probe spacing, i.e. $L \gg S$ and $W \gg S$ so that the sheet resistace is $R_s \equiv R_s^{\infty}$. By varying the length and width of the samples, measuring the sheet resistance and comparing it to R_s^{∞}, a calibration test is performed. Knowing the electrode sample width and length, it can be interpolated that $C \approx 0.43$. The sheet resistivity ϱ is then given by $\varrho = R_s\delta$, where δ is the sample thickness. The surface electric conductivity is simply given by $\sigma = \varrho^{-1}$.

Table 1 Properties of PEDOT: PSS films.

Film type	IL [wt%]	Sheet Resistance [Ω]	Conductivity [S·cm^{-1}]
Thin Film (~24 µm)	0	NA	NA
	15	3.9975	104.23

	30	1.5200	274.13
	45	1.8466	225.64
	60	1.6318	255.35
Thick Film (~142 µm)	0	21.8834	3.22
	15	1.0469	67.27
	30	0.7151	98.48
	45	0.9898	71.15
	60	0.5405	130.28

The measured sheet resistance and electric conductivity are given in **Table 1**. A noticeable value is the pure PEDOT: PSS thick film, which is the highest registered, but still relatively low. Even though it could be considered satisfactory, this film is so brittle that it could not be used as a cathode or any similar purpose.

The 1-butyl- 3-methylimidazolium octyl sulfate ionic liquid increased the conductivity, e.g., of the films of two orders of magnitude in case of the thick films. Moreover, the IL also enhanced the mechanical properties since, with the higher concentrations of IL, more robust and stretchable films were obtained. This is a result of the IL's screening effect explained by a higher crystallinity and interconnection of the PEDOT nanofibrillar structures, which has been demonstrated by UV-vis-NIR spectra, Raman spectra and AFM phase images of PEDOT:PSS films as a function of ionic additives [21]. This is the main reason behind the increase in conductivity. The thick film shows a lower sheet resistance, probably because the thick film appears to be more compact (see SEM images in Fig. 2). However, as the formula for the electric conductivity shows (see earlier), the much higher thickness results into a lower electric conductivity of the thicker film. Furthermore, it is suspected that the IL molecules are mostly present in the more disordered regions due to the increased PEDOT crystallinity, which gives rise to a nanofiber network embedded in a soft matrix. This structure is responsible for the high elasticity and softening of the material, in agreement with [21].

From **Table 1**, the thick and thin formulations with 60 wt% of IL were chosen to be tested as the cathode in the battery due to their value of conductivity. Furthermore, they possessed better compactness, and they were the easiest to spread and the most flexible and bendable ones.

The surface morphologies of the PEDOT:PSS films were first characterised using SEM images. **Fig. 2** shows SEM images of the thick and thin film with 60 wt% of IL, the thick and thin films present quite smooth surface aside from few agglomerations. The sample surface compositions were compared using energy-dispersive X-ray spectroscopy (EDS). The PEDOT:PSS films surface exhibit majoritarily C (Carbon), O (Oxygen) and S (Sulfur) contents on different spots, two of which are shown in **Fig. 2** (b) and (d), which indicates quite small impurities and quite high homogeneity of the films.

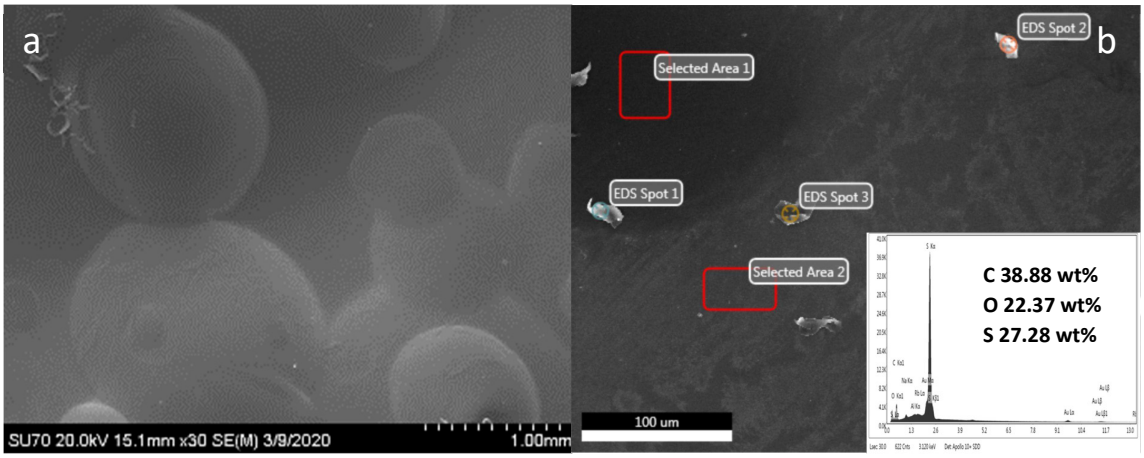

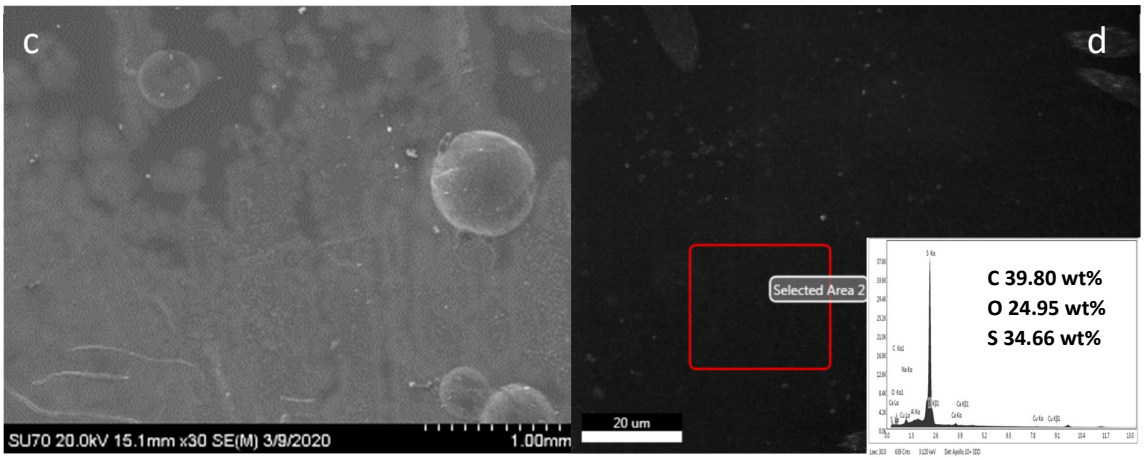

Fig. 2 SEM images and EDS results of thick(a,b) and thin(c,d) film with 60% of IL.

Fig. 3 shows FTIR profiles of: a pure PEDOT:PSS film, the pure ionic liquid and the PEDOT:PSS film with 60 wt% of IL. The FTIR analyses help to determine whether some new chemical structures are created. What can be seen is that the spectra are very similar, and that the only difference is in the intensity of the peaks. The similarity proves that there is indeed no chemical reaction between the ionic liquid and PEDOT or PSS, just as it was suggested by Wang et al. [21].

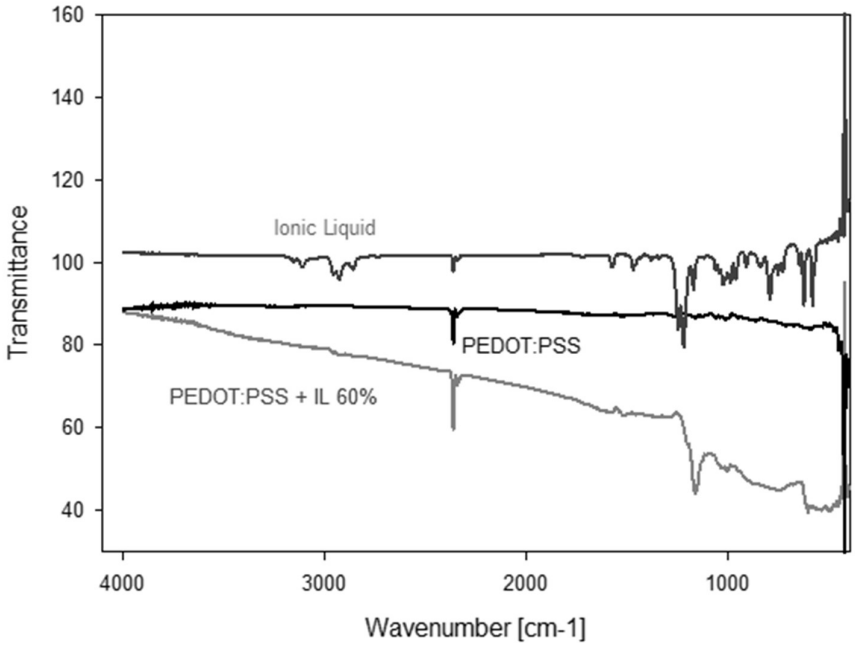

Fig. 3 FTIR profiles of PEDOT:PSS film with 60% of IL, pure PEDOT:PSS film and Ionic liquid.

To characterise the electrochemical performances of the battery, thin and thick films with 60 wt% of IL were inserted in the sandwich structure and tested as described in the methodology above. **Fig. 4** and **Fig. 5** show the discharge curves of the two types of cell at two current densities: 0.8 $mA \cdot cm^{-2}$ and 4 $mA \cdot cm^{-2}$. The initial voltage drops as a result of polarisation phenomena occurring during the assembly of the battery. The resulting discharge curves are not perfectly linear and horizontal due to various imperfections related to assembly and connections, but the standard features indicate that they are working as batteries.

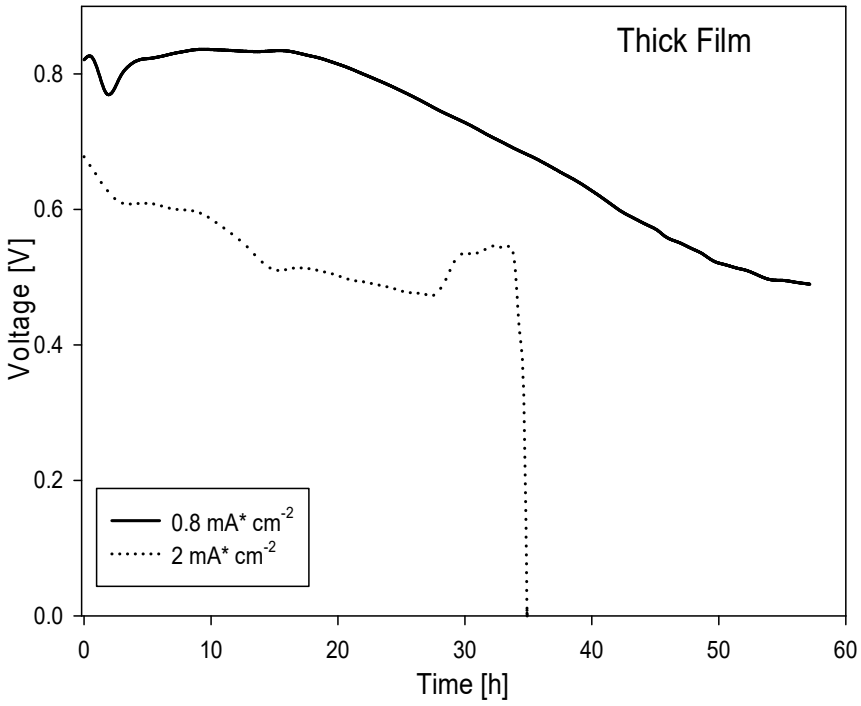

Fig. 4 Discharge curves of thick film battery at two current densities: 0.8 mA·cm^{-2} and 4 mA·cm^{-2}.

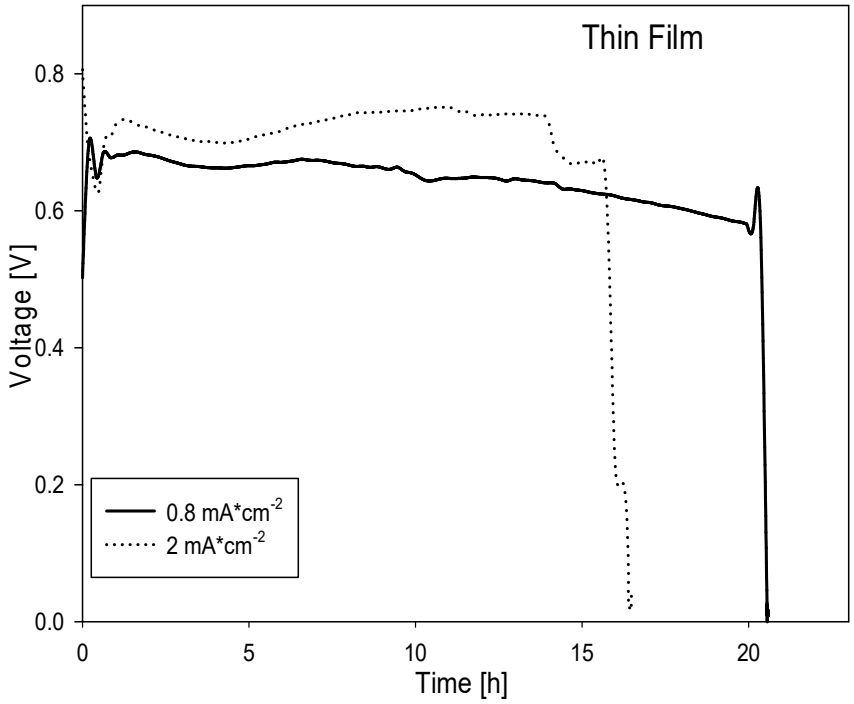

Fig. 5 Discharge curves of thin film battery at two current densities: 0.8 mA·cm^{-2} and 4 mA·cm^{-2}.

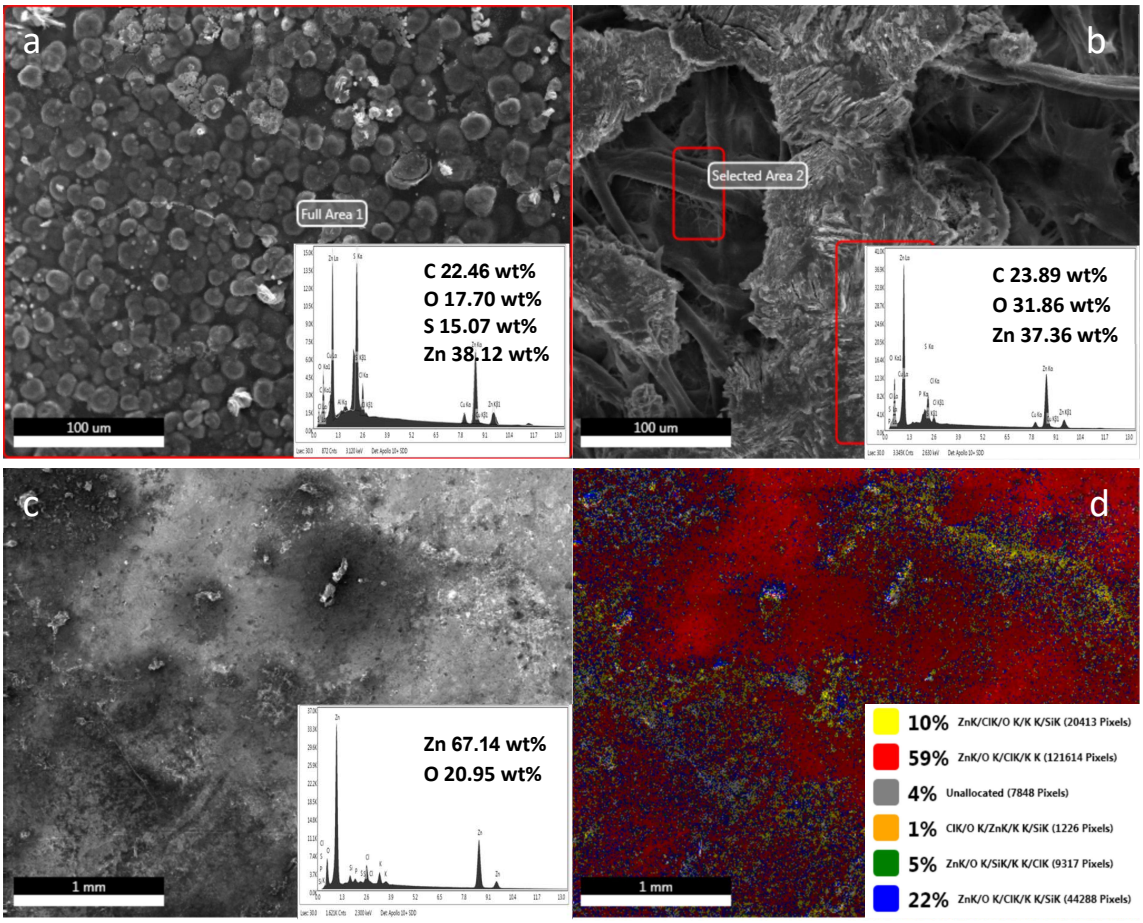

Fig. 6 After discharge SEM and EDS analysis: (a) PEDOT:PSS thick film, (b) separator and (c,d) zinc anode.

After discharge, the batteries were opened, and each element of the stack was analysed with SEM and EDS. **Fig. 6** shows these SEM/EDS results, where **Fig. 6**(a) and (b) present the results of the PEDOT:PSS thick film and separator, respectively. It is clearly seen that a new shape appeared on the surface of the electrode. Comparing the PEDOT: PSS EDS spectra in **Fig. 6** with those in **Fig. 2**, we can see that the oxygen content has increased, and a new peak, belonging to Zn, appears. This leads to the conclusion that zinc-oxide particles are present on the cathode. The separator shows two distinct areas. The first is a fibre-like structure for which the EDS shows predominantly carbon and oxygen peaks, which are the components of cellulose. The second shows zinc and oxygen peaks, indicating the presence of some ZnO. ZnO's presence on both the PEDOT:PSS film and the separator warrant the conclusion that the ions actually migrate through the separator pores so that the metal-air electrochemical reactions are indeed occurring. Then, also the anode (**Fig. 6** c,d) was analysed. The obtained results show Zinc and Oxygen's predominance on the discharged electrode's surface, just as we expected. The other elements found on the electrode's surface are Cl, K and small traces of Si. Chlorine and Potassium are elements in the electrolyte used (PBS), so it is not questionable to find them in small quantities on the surface. **Fig. 6** (d) represents a colour map with different electrode surface areas where concentrations of different elements are found. This inhomogeneity of the distribution is due to a non-homogeneous consumption of the electrode and therefore makes it clear that the contact between the various layers of the battery is not perfect and must undoubtedly be improved. Looking closer, the most widespread areas (red and blue), almost only Zinc and Oxygen are observed on the surface. This result confirms the idea that the battery is a zinc-air battery and that the predominant reactions are those between atmospheric oxygen and zinc.

Table 2 Discharge characteristics of the batteries.

Type	Current Density [mA·cm^{-2}]	Discharge time[h]	Average voltage at plateau [V]	Capacity [mA·h]	Volumetric Power density [mW·cm^{-3}]	Volumetric Energy density [mW·h·cm^{-3}]
Thin film	0.8	~21	~0.66	4.2	8.05	169.05
	4	~16	~0.72	16	44.42	710.72
Thick film	0.8	>57	~0.82	11.4	8.53	486.21
	4	~35	~0.60	35	30.51	1067.85

To evaluate the practical performance of the battery, the discharge characteristics of the batteries are presented in **Table 2**. The assembled stacks exhibited voltages between 0.6 - 0.8 V and had lifetimes longer than 57 h at 0.8 mA·cm^{-2} current density for the thick film. It is clear that the film thickness influences the performances of the battery, having better behaviour for thin film stacks but shorter discharge time in comparison with the thick film batteries. It should be noted that, although the thin film showed a higher electric conductivity, a thicker film will allow for more contact with the PEDOT catalyst sites and therefore for a higher formation of active species, which finally results into more delivered energy for the thick film. This can be explained in more detail when looking to the redox reactions that are happening for the Zn-air battery. The oxygen from the air is reduced at the PEDOT:PSS cathode, releasing hydroxyl ions that diffuse through the electrolyte towards the zinc anode where it oxydizes zinc to zinc oxide [12]. The reaction occurring at the PEDOT:PSS cathode is represented by $O_2 + 2H_2O + 4e^- \rightarrow 4OH^-$, with a standard cathode electrode potential at 25 °C of $E_c^0 = 0.4\,V$, whereas at the Zn anode the following reaction occurs $Zn + 2OH^- \rightarrow ZnO + H_2O + 2e^-$, with a standard anode electrode potential at 25 °C of $E_a^0 = -1.25\,V$. The equilibrium standard potential is given by $E_{eq} = E_c^0 - E_a^0 = 1.65\,V$. It is easy to see that the total reaction is $2Zn + O_2 \rightarrow 2ZnO$, but the role of the hydroxyl ion is crucial as it also serves to close the electric circuit loop. As $E_{eq} > 0$, it is a spontaneous reaction, delivering a current. It can therefore be understood that a thicker PEDOT-electrode will enhance such reactions, because of a higher number of contact sites in the pores of the PEDOT:PSS. Apparently, the balance between the reduction in the electric conductivity and possible overpotential losses on one side and the increase of catalyst contact sites on the other tilt towards a better battery performance with the thick film. Let us note that the working voltage on discharge is quite lower than the theoretical 1.65 V, being typically less than 1.2 V [12]. The measured voltage is lower than this one, most probably due to the internal loss of the cell, ohmic and concentration losses (overpotential). The influence of the electrolyte should also be taken into account. The PBS contains chloride ions which may cause overpotential accompanying the side reaction $Zn \rightarrow Zn^{2+} + 2e^-$ [22]. As such a voltage, shown by the discharge curves, is amply sufficient for the purposes of monitoring medical devices, this is not a problem. Improving the setup to reduce the several aforementioned losses would result into unnecessary higher costs. On a side note, the polymeric layer of PEDOT:PSS not only acts as a catalyst but may also show side reactions in the process, where reversible reductions and oxidations are reported in the literature by means of visible and NIR spectra [23], [24].Nevertheless, the thin film shows appreciable performances for a thickness of just 24 µm. These batteries system also delivered a maximum volumetric power density of 7.97 mW·cm^{-3}, and a maximum energy density of 259.07 mW·h·cm^{-3} could be generated. Generally, the power requirements of active IMDs fall in the level of micro- to milliwatts [25]. PEDOT:PSS as a cathode in a Zn-air battery could become a cost-effective power source for some IMDs, such as endoscopy capsules. Higher power output can be achieved using devices connected in series. **Fig. 7** shows three cells placed in series, being able to power a 2.5V LED for more than four hours.

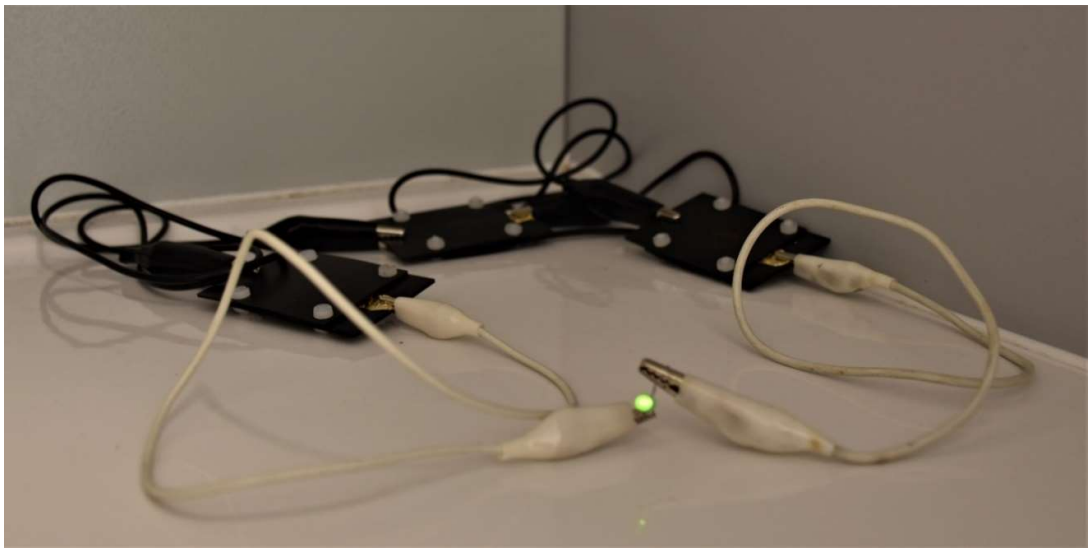

Fig. 7 Series of three batteries connected to power a 2.5V LED.

The results have shown battery characteristics that are sufficient for supplying power to medical monitoring devices. As the future purpose is to implement such studies as wearable devices, let us assess the possibility that the battery in this work is wearable. We propose three main criteria. The first is weight, the second biocompatibility and the third is a minimum of flexibility. It was measured that a whole battery setup weighs around 3 g, which obviously does not cause any difficulties for the patient to wear. The biocompatibility of the PEDOT:PSS [26] means that such a hydrogel would not cause any difficulties when worn on the skin. Should such a battery be incorporated in clothing, its small size would allow its positioning relatively easily. In order to perform the characterisation tests, the battery was placed between PLA plates. However, it should be noted that in its application the battery will be incorporated in, for instance, a wound dressing, which is englobed by flexible hydrogels. This brings us to assessing the flexibility of the electrodes. Flexibility tests have shown that small curvatures (such as on an arm) do not pose any difficulty for the functioning of the battery. These observations, although further development is necessary, along with the energetic characteristics show that the battery studied in this paper is quite viable as a wearable battery.

4. Conclusions

This research project's primary aim was to explore the possibility of building energy storage systems that would be easy to fabricate, cost-effective, and have the potential for miniaturisation. Different configurations were taken into consideration, and finally, it was decided to develop a Zn-air battery for its great potential, low cost and resistance to aqueous electrolytes. As cathode, PEDOT:PSS films was taken in consideration for its suitability as a conductive, stable and easy-to-handle polymeric material.

The results presented in this work indicate a promising approach to the fabrication of miniaturised biocompatible batteries employing a stable and low-cost metal anode, biocompatible conducting polymer cathode, and body fluid as the electrolyte. With a layered structure, with a volume of ~20 mm^3, and a full battery thickness of ~2 mm, the battery can generate a voltage up to 0.8 V and deliver a maximum output power of 550 µW. The battery would occupy minimal space and would be easy to build with a first cost of less than ~ 20 €/g, as demonstrated. Moreover, this configuration produces a power of the order of 10^{-2} mW and a duration of several hours, so could already be used to power some implantable and wearable medical devices.

Acknowledgements

This research has received funding from the European Union H2020 Programme under Grant agreement number 785219: Graphene Flagship and PRODEX EVAPORATION of the Belgian Science Policy Office - BELSPO. G. Wallaert from the “Materials engineering, characterization, synthesis and recycling” group at ULB is thanked for his technical assistance for the SEM(EDS) images and profilometry tests.

References

[1] K. Diaconu, Y. F. Chen, C. Cummins, G. Jimenez Moyao, S. Manaseki-Holland, and R. Lilford, "Methods for medical device and equipment procurement and prioritization within low- and middle-income countries: Findings of a systematic literature review," *Globalization and Health*, vol. 13, no. 1, pp. 1–16, 2017, doi: 10.1186/s12992-017-0280-2.

[2] N. M. Elman, H. L. Ho Duc, and M. J. Cima, "An implantable MEMS drug delivery device for rapid delivery in ambulatory emergency care," *Biomedical Microdevices*, vol. 11, no. 3, pp. 625–631, 2009, doi: 10.1007/s10544-008-9272-6.

[3] A. J. Chung, Y. S. Huh, and D. Erickson, "A robust, electrochemically driven microwell drug delivery system for controlled vasopressin release," *Biomedical Microdevices*, vol. 11, no. 4, pp. 861–867, 2009, doi: 10.1007/s10544-009-9303-y.

[4] M. Southcott *et al.*, "A pacemaker powered by an implantable biofuel cell operating under conditions mimicking the human blood circulatory system-battery not included," *Physical Chemistry Chemical Physics*, vol. 15, no. 17, pp. 6278–6283, 2013, doi: 10.1039/c3cp50929j.

[5] C. A. da Costa, C. F. Pasluosta, B. Eskofier, D. B. da Silva, and R. da Rosa Righi, "Internet of Health Things: Toward intelligent vital signs monitoring in hospital wards," *Artificial Intelligence in Medicine*, vol. 89, no. May, pp. 61–69, 2018, doi: 10.1016/j.artmed.2018.05.005.

[6] Z. Li, G. Zhu, R. Yang, A. C. Wang, and Z. L. Wang, "Muscle-driven in vivo nanogenerator," *Advanced Materials*, vol. 22, no. 23, pp. 2534–2537, 2010, doi: 10.1002/adma.200904355.

[7] H. Cao *et al.*, "An implantable, batteryless, and wireless capsule with integrated impedance and pH sensors for gastroesophageal reflux monitoring," *IEEE Transactions on Biomedical Engineering*, vol. 59, no. 12 PART2, pp. 3131–3139, 2012, doi: 10.1109/TBME.2012.2214773.

[8] L. Halámková, J. Halámek, V. Bocharova, A. Szczupak, L. Alfonta, and E. Katz, "Implanted biofuel cell operating in a living snail," *Journal of the American Chemical Society*, vol. 134, no. 11, pp. 5040–5043, 2012, doi: 10.1021/ja211714w.

[9] C. Wang *et al.*, "Recent progress of metal-air batteries-A mini review," *Applied Sciences (Switzerland)*, vol. 9, no. 14, pp. 1–22, 2019, doi: 10.3390/app9142787.

[10] S. Stauss and I. Honma, "Biocompatible batteries-materials and chemistry, fabrication, applications, and future prospects," *Bulletin of the Chemical Society of Japan*, vol. 91, no. 3, pp. 492–505, 2018, doi: 10.1246/bcsj.20170325.

[11] J. Fu, Z. P. Cano, M. G. Park, A. Yu, M. Fowler, and Z. Chen, "Electrically Rechargeable Zinc–Air Batteries: Progress, Challenges, and Perspectives," *Advanced Materials*, vol. 29, no. 7, 2017, doi: 10.1002/adma.201604685.

[12] P. Gu, M. Zheng, Q. Zhao, X. Xiao, H. Xue, and H. Pang, "Rechargeable zinc-air batteries: A promising way to green energy," *Journal of Materials Chemistry A*, vol. 5, no. 17, pp. 7651–7666, 2017, doi: 10.1039/c7ta01693j.

[13] R. Cao, J. S. Lee, M. Liu, and J. Cho, "Recent progress in non-precious catalysts for metal-air batteries," *Advanced Energy Materials*, vol. 2, no. 7, pp. 816–829, 2012, doi: 10.1002/aenm.201200013.

[14] B. Li *et al.*, “Eggplant-derived microporous carbon sheets: Towards mass production of efficient bifunctional oxygen electrocatalysts at low cost for rechargeable Zn-air batteries,” *Chemical Communications*, vol. 51, no. 42, pp. 8841–8844, 2015, doi: 10.1039/c5cc01999k.

[15] V. G. Khomenko, V. Z. Barsukov, and A. S. Katashinskii, “The catalytic activity of conducting polymers toward oxygen reduction,” *Electrochimica Acta*, vol. 50, no. 7–8, pp. 1675–1683, 2005, doi: 10.1016/j.electacta.2004.10.024.

[16] B. Winther-Jensen, O. Winther-Jensen, M. Forsyth, and D. MacFarlane, “High Rates of Oxygen Reduction,” *Science*, vol. 321, no. 1, pp. 671–674, 2008.

[17] Y. L. Kuo, C. C. Wu, W. S. Chang, C. R. Yang, and H. L. Chou, “Study of Poly (3,4-ethylenedioxythiophene)/MnO<inf>2</inf> as Composite Cathode Materials for Aluminum-Air Battery,” *Electrochimica Acta*, vol. 176, pp. 1324–1331, 2015, doi: 10.1016/j.electacta.2015.07.151.

[18] J. Tarver, J. E. Yoo, and Y.-L. Loo, “Comprehensive Nanoscience and Technology,” *Comprehensive Nanoscience and Technology*, pp. 413–446, 2011.

[19] E. Nasybulin *et al.*, “Electrocatalytic properties of poly(3,4-ethylenedioxythiophene) (PEDOT) in Li-O2 battery,” *Electrochemistry Communications*, vol. 29, pp. 63–66, 2013, doi: 10.1016/j.elecom.2013.01.011.

[20] D. H. Yoon, S. H. Yoon, K. S. Ryu, and Y. J. Park, “PEDOT:PSS as multi-functional composite material for enhanced Li-air-battery air electrodes,” *Scientific Reports*, vol. 6, no. January, pp. 1–9, 2016, doi: 10.1038/srep19962.

[21] Y. Wang *et al.*, “A highly stretchable, transparent, and conductive polymer,” *Science Advances*, vol. 3, no. 3, pp. 1–11, 2017, doi: 10.1126/sciadv.1602076.

[22] A.R. Mainar, E. Iruin, L.C. Colmenares, A. Kvasha, I. de Meatza, M. Bengoechea, O. Leoret, I. Boyano, Z. Zhang, J.A. Blazquez, “An overview of progress in electrolytes for secondary zinc-air batteries and other storage systems based on zinc,” *Journal of Energy Storage*, vol. 15, pp. 304-328, 2018, doi: 10.1016/j.est.2017.12.004.

[23] C. Zhu, J. Zhai, D. Wen, and S. Dong, “Graphene oxide/polypyrrole nanocomposites: One-step electrochemical doping, coating and synergistic effect for energy storage,” *Journal of Materials Chemistry*, vol. 22, no. 13, pp. 6300–6306, 2012, doi: 10.1039/c2jm16699b.

[24] M. Marzocchi *et al.*, “Physical and Electrochemical Properties of PEDOT:PSS as a Tool for Controlling Cell Growth,” *ACS Applied Materials and Interfaces*, vol. 7, no. 32, pp. 17993–18003, 2015, doi: 10.1021/acsami.5b04768.

[25] D. Jiang *et al.*, “A 25-year bibliometric study of implantable energy harvesters and self-powered implantable medical electronics researches,” *Materials Today Energy*, vol. 16, p. 100386, 2020, doi: 10.1016/j.mtener.2020.100386.

[26] D. Fichou, G. Horowitz, “Molecular and polymer semiconductors, conductors, and superconductors: overview,” *Encycl. Mater. Sci. Technol.,* pp. 5748–5757, 2001, doi: 10.1016/B0-08-043152-6/01000-7